Investigating the oxidation of dimethyl ether and dimethyl ether/hydrogen mixtures by chemical kinetic modeling

Ákos Veres-Ravai[a,b*], István Gyula Zsély[a], Máté Papp[a], Tamás Turányi[a]

[a]Institute of Chemistry, ELTE Eötvös Loránd University, Budapest, Hungary
[b]ELTE Hevesy György PhD School of Chemistry, Budapest, Hungary

Abstract

Dimethyl ether (DME, CH_3OCH_3) can be produced from biomass or synthesized with H_2 from renewable sources and captured CO_2. It is an attractive alternative to conventional diesel fuel for compression-ignition engines. To facilitate its application, chemical kinetic models are needed to describe the combustion of DME under typical conditions of applications. The aim of this work is to make a quantitative comparison of recent detailed DME oxidation mechanisms on a comprehensive experimental data set. 18 detailed DME oxidation mechanisms were collected from the literature in CHEMKIN format. The experimental data (33149 data points in 1252 data series) collected from 98 articles were encoded in ReSpecTh Kinetic Data format XML files. The chemical kinetic simulations were performed with the program *Optima++* and the solver packages Cantera and *OpenSMOKE++*. The performances of the reaction mechanisms were compared quantitatively on a wide range of DME and DME-H_2 oxidation experiments including concentration measurements in jet-stirred reactor (JSR), flow reactor (FR) and burner-stabilized flames (BSF), ignition delay time measurements in shock tube (ST) and rapid compression machine (RCM), and laminar burning velocity measurements. The experiments cover wide ranges of equivalence ratio, pressure and temperature. Ignition delay time and laminar burning velocity measurements could be reproduced well by the models, while we have worse results for the concentration measurements. The performance of the models reproducing experimental data was analysed according to experiment types and conditions using quantitative measures. The simulation results for JSR and FR measurements can be sensitive to the temperature used in the calculations, so the effect of experimental temperature uncertainty was also considered. Local sensitivity analysis was performed to identify the most important reactions in the best-performing model. The results can be used in further mechanism development work.

Keywords: dimethyl ether; combustion kinetic modeling; mechanism development

*Corresponding author.

1. Introduction

As the global demand for cleaner and more sustainable energy sources grows, dimethyl ether (DME) has emerged as a promising alternative fuel. DME is a versatile, non-toxic, and easily liquefiable compound that can be derived from renewable sources such as biomass, as well as from natural gas and coal. With its high cetane number, DME is a viable substitute for diesel oil in compression ignition engines. Additionally, the combustion of DME produces significantly lower emissions of particulate matter and nitrogen oxides compared to conventional fossil fuels, contributing to improved air quality and reduced environmental impact [1]. Its compatibility with existing LPG infrastructure further enhances its potential for widespread adoption in transportation and industrial applications.

Due to its increasing importance, several experimental investigations have been carried out and detailed reaction mechanisms describing DME combustion have been developed in the last two decades. However, the performance of these mechanisms on simulating the experiments is mostly insufficient, and significant discrepancies in the simulation results are obtained. Thus, further investigation and development of these mechanisms are necessary.

In this work, the performance of 18 detailed reaction mechanisms was quantitatively assessed based on how well they reproduced the results of published experimental data. The method developed by Turányi et al. [2] was used to compare and quantify the performance of the mechanisms. Ignition delay times measured in shock tubes (ST) and rapid compression machines (RCM), and concentration measurements carried out in jet stirred reactors (JSR), flow reactors (FR) and burner-stabilized flames (BSF), as well as laminar burning velocity (LBV) measurements were collected from the available publications. Using the overall best model, local sensitivity analysis was performed to identify the most important reactions of the DME combustion process.

2. Experimental data collection

Our aim was to collect a large set of experimental data on DME combustion. The summary of the experimental data with conditions is given in Table 1. Besides neat DME, the mixtures containing hydrogen and/or carbon monoxide were also included in the present study.

All collected indirect experimental data (33149 data points in 1252 data series of 98 experimental articles) were encoded in ReSpecTh Kinetics Data (RKD) v2.5 files.

The RKD format [3] is XML-based and can be read well by both humans and computer programs. The RKD-format files were created with our Optima++ code [4]. *Optima++* was also used for reading the data files, running *Cantera* [5] and *OpenSMOKE++* [6], which were the two solvers used in the study, and comparing the simulation results with the experimental data.

Table 1 The collected experimental data and their experimental conditions. Abbreviations and notations: FR: flow reactor; JSR: jet-stirred reactor; BSF: burner-stabilized flame; ST: shock tube; RCM: rapid compression machine; c_{out}: outlet concentration; IDT: ignition delay time; LBV: laminar burning velocity; T: (cold-side) temperature; p: pressure; φ: equivalence ratio

Experimental method	Measured data	number of data points / data series / XMLs	T / K	p / atm	φ
FR	c_{out}	18334/357/56	298 – 1458	1.0 – 59.2	pyrol. – 59.1
FR	conc.-time	68/4/1	980	10.0	pyrol.
JSR	c_{out}	2444/161/23	395 – 1275	0.9 – 100.0	0.17 – 2.00
BSF	c_{out}	9259/367/31	295 – 740	0.03 – 1.00	0.67 – 2.21
ST	IDT	1538/173/173	607 – 1657	0.7 – 51.8	0.43 – 2.00
RCM	IDT	477/61/61	610 – 1670	1.0 – 60.1	0.30 – 5.00
laminar flame	LBV	1029/129/129	285 – 650	0.4 – 19.9	0.49 – 2.13

3. Comparison of the performance of the mechanisms

Experimental data were reproduced using detailed reaction mechanisms that are either widely used for several fuels or were developed exclusively for the description of DME combustion. All collected experimental data were simulated with each reaction mechanism. *Cantera* was used primarily as a solver to carry out the simulations, while *OpenSMOKE++* was used to simulate flow reactor measurements.

The obtained simulation results, belonging to different mechanisms, were typically different from each other and sometimes also from the experimental data. Two typical examples of the behaviour of the mechanisms can be seen in Figure 1.

Agreement of the simulation results with the experimental data was investigated comprehensively using the following error function:

$$E = \frac{1}{N}\sum_{f=1}^{N_f}\sum_{s=1}^{N_{fs}}\frac{1}{N_{fsd}}\sum_{d=1}^{N_{fsd}}\left(\frac{Y_{fsd}^{\mathrm{sim}} - Y_{fsd}^{\mathrm{exp}}}{\sigma(Y_{fsd}^{exp})}\right)^2 \qquad (1)$$

In equation (1), N is the number of experimental data series in the data collection, N_f is the number of datasets (i.e. the number of RKD files), N_{fs} is the number of data series in dataset f, and N_{fsd} is the number of data points in data set f and data series s. y_{fsd}^{sim} and y_{fsd}^{exp} are the simulated and experimental values of the d-th experimental data point of the s-th data series in the f-th dataset. $\sigma(Y_{fsd}^{\text{exp}})$ is the estimated standard deviation of the data point y_{fsd}^{exp}. The corresponding simulated value y_{fsd}^{sim} is obtained from a simulation using a detailed mechanism and an appropriate simulation method. If a measured value is

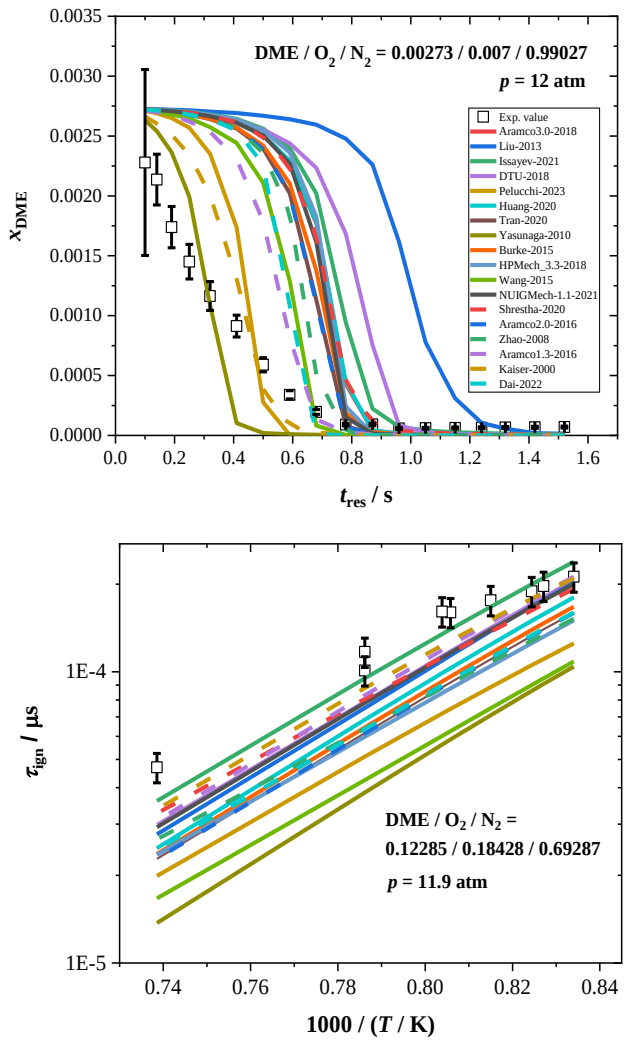

Figure 1 Comparison of the experimental values and the corresponding simulation results using two example datasets. a) concentration measurements in a flow reactor by Curran et al. [7]; b) ignition delay times measured in a shock tube by Burke et al. [8].

characterized by absolute errors (the scatter is independent of the magnitude of y_{fsd}), then $Y_{fsd} = y_{fsd}$. If the experimental results are described by relative errors (the scatter is proportional to the value of y_{fsd}), then option $Y_{fsd} = \ln(y_{fsd})$ is used.

When estimating the standard deviation of the data points, both uncertainty $\sigma_{\text{exp,fsd}}$ provided by the authors of the publications or estimated in this study, and the $\sigma_{\text{stat},i}$ statistical scatter of the data points were considered:

$$\sigma_{fsd} = \sqrt{\sigma_{\text{exp},fsd}^2 + \sigma_{\text{stat},fs}^2} \qquad (2)$$

For the flow reactor and jet-stirred reactor measurements, the measured temperature values are uncertain and the simulation results can be sensitive to the temperature used in the calculations, so the effect of experimental temperature uncertainty was also considered. When estimating the standard deviation of the data points, an additional $\sigma_{unc,fsd}^2$ variance term, calculated using the error propagation formula, was added to Equation (2) to consider the experimental temperature uncertainty:

$$\sigma_{fsd} = \sqrt{\sigma_{\text{exp},fsd}^2 + \sigma_{\text{stat},fs}^2 + \sigma_{\text{unc},fsd}^2} \qquad (3)$$

The performance of a mechanism can be considered good if $E < 9$ is fulfilled, which means the experimental values were reproduced within the 3σ standard deviation limits of the data series on average. The error function values calculated using all the experimental data and some subsets based on the experiment types are shown in Table 2.

The table, however, does not contain all the collected data points. To avoid biased conclusions, those points were excluded from comparison, for which the error function value was greater than 9 for all models, indicating that no mechanism could simulate them properly. Those data points for which the simulations failed for at least one of the mechanisms were also excluded. The number of failed simulations, along with the remaining data points, are also shown in Table 2. As can be seen, the number of failed simulations is especially high for Shrestha-2020, but negligible compared to the number of total collected data.

As can be seen in Table 2, the overall best-performing mechanism is HPMech3.3-2018. It is, however, only under the desirable E value ($E = 9$) for the shock tube experiments. In general, most mechanisms perform worse than this for most experiment types, as there are E values under 9 only for shock tube (most mechanisms), laminar burning velocity (NUIGMech1.1-2021) and flow-reactor concentration-time profile measurements (Yasunaga-2010).

Table 2 Comparison of the investigated reaction mechanisms based on the error function values *E* calculated for all experimental data and various subsets of them. The final order in this table is based on the overall error function values. In the table, FR-OC refers to outlet concentrations, while FR-CT refers to concentration-time profiles measured in the flow reactor. The number of unsuccessful simulations is also indicated.

		JSR	FR-OC	FR-CT	ST	RCM	BSF	LBV	Overall	Failed
Number of data series		157	352	4	167	61	340	129	1210	
Number of data points		2130	15097	42	1290	392	7146	958	27055	
HPMech3.3-2018	[9]	18.2	70.6	122.5	6.5	14.1	55.9	16.2	21.7	5
Zhao-2008	[10]	32.4	72.1	146.7	10.8	19.9	40.7	11.2	22.6	25
Dai-2022	[11]	44.5	36.0	139.4	9.3	38.6	37.4	24.9	24.4	2
Aramco2.0-2016	[12]	37.3	76.6	137.8	4.5	26.7	86.8	17.2	26.5	1
Wang-2015	[13]	18.9	37.7	107.7	14.8	16.9	45.0	43.7	28.1	17
Burke-2015	[8]	34.1	104.6	137.8	4.5	15.2	73.3	21.8	28.6	2
Aramco3.0-2018	[14]	21.0	119.3	216.2	5.3	18.1	88.8	12.8	29.0	1
NUIGMech1.1-2021	[15]	14.1	106.7	214.8	5.6	24.3	147.7	8.6	30.5	2
Pelucchi-2023	[16]	71.7	44.3	41.8	6.3	48.2	25.1	49.1	32.7	11
Aramco1.3-2013	[17]	49.3	111.9	237.7	5.7	36.9	102.3	18.6	34.6	0
Tran-2020	[18]	37.4	78.7	137.8	4.5	26.5	86.8	82.8	44.9	3
Shrestha-2020	[19]	72.2	120.9	171.9	27.7	15.5	17.6	80.6	53.9	156
Liu-2013	[20]	34.0	288.4	135.5	27.4	20.6	32.2	10.2	54.0	19
Kaiser-2000	[21]	29.6	70.6	226.5	7.2	17.1	16.1	146.7	56.9	19
Huang-2021	[22]	24.5	131.8	216.2	5.3	17.8	89.8	117.7	59.9	5
Issayev-2021	[23]	72.1	162.1	249.9	7.4	15.5	74.8	104.5	61.8	18
DTU-2018	[24]	255.1	212.6	112.9	18.2	150.7	15.0	22.5	71.9	17
Yasunaga-2010	[25]	48.9	116.3	6.8	16.2	39.4	174.7	197.2	92.6	11

Zhao-2008 and Dai-2022 are the second and third best models, respectively, with overall *E* values under 25, and four more mechanisms are under 30. As these are the lowest values, the results also indicate that the mechanisms cannot reproduce the experimental data within their 3σ uncertainty range on average, meaning that further development of the models is necessary.

It is also useful to use stacked bar plots of errors to compare the mechanisms. This can be seen in Figure 2, where the distribution of the error function values is visualized. It shows the frequencies of data points that were reproduced by the mechanisms within a given threshold of the multiple of the estimated standard deviation. Here, the error function values were not considered, only the count of them within the thresholds. Therefore, it resulted in a different order than Table 2 based on the average error function value.

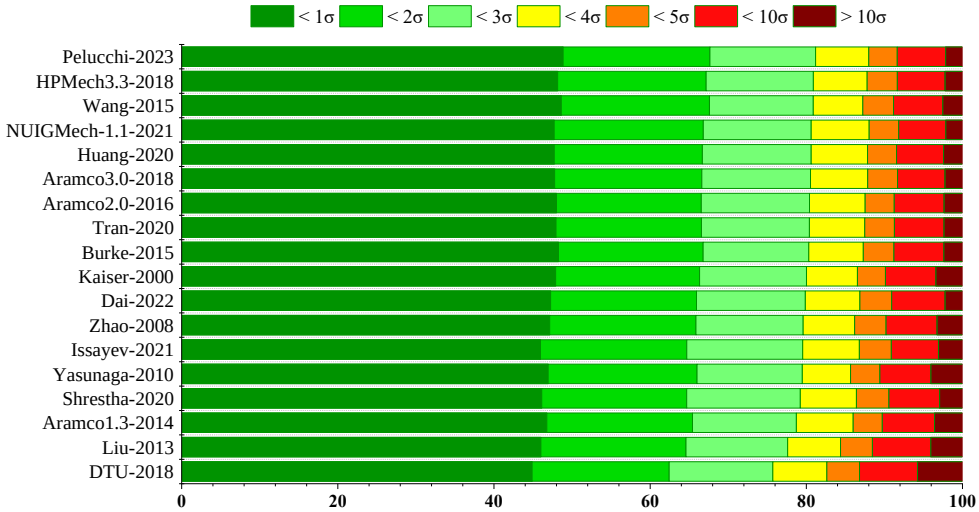

Figure 2 Stacked bar plot of the frequencies of the reproduction of data points within given multiples of the estimated standard deviations of the data. The final order in the figure is based on the "$< 3\sigma$" values.

The stacked bar plot shows that there are no great differences between the mechanisms in the percentages as they reproduce the data points in different uncertainty ranges. Based on this comparison, Pelucchi-2023 performs the best, reproducing 81.19% of the data points within 3σ uncertainty. HPMech3.3-2018, the best model by overall average E value, is the second best here with 80.91% of the data points under 3σ, while Wang-2015 is the third one with 80.89%. The results show that most data points considered in the comparison are reproduced within the desirable uncertainty range, however, about 20-25% percent of the data points are not, and these lead to the high average values in Table 2. In optimization work, it would be desirable to improve the description of these data points as well.

4. Results of the sensitivity analysis

Local sensitivity analysis [26] was carried out with the HPMech3.3-2018 mechanism using 4464 data points to identify the most important reactions in the best-performing model. For the flow reactor, jet-stirred reactor and burner-stabilized flame measurements, only the concentration changes of DME are considered. For the shock tube ignition delay time and laminar burning velocity measurements, we experienced high running times for several XMLs and due to this, only a few experimental data points were chosen from these files to complete the sensitivity analysis.

The sensitivity coefficients of the measured values with respect to the +5% relative perturbation of A preexponential Arrhenius parameters for each reaction were investigated. Table 3 shows the first 10 reactions with the highest frequencies of significant sensitivities from the considered mechanism for each experiment type. A sensitivity coefficient is considered significant if its normalized absolute value is greater than 10% of the highest absolute normalized sensitivity coefficient of this data point. The frequency values (the freq. columns in Table 3) show the ratio of these important data points to all data points. The $|\widetilde{sn}|_j$ values in Table 3 are the mean scaled absolute normalized sensitivity coefficients:

$$|\widetilde{sn}|_j = \frac{1}{N_i}\sum_{i=1}^{N_i}\frac{|sn_{ij}|}{\max|sn|_i} \qquad (4)$$

Here, i is the index of the data point, and j is the index of the reaction (A parameter) in the mechanism. The scaling of the normalized sensitivity coefficients described with Equation (4) was done by dividing with the maximum sensitivity coefficient of the data point.

Based on the sensitivity analysis results of Table 3, the most important reactions of HPMech3.3-2018 are largely dependent on the experiment type, however, there are certain reactions that are present for most types. The reaction $CH_3OCH_3+HO_2=CH_3OCH_2+H_2O_2$, when DME reacts with the hydroperoxyl radical, is the most important step for the flow reactor outlet concentration measurements, but also in the top 3 for jet-stirred reactor and ignition delay time measurements. The reaction of DME with the hydroxyl radical, $CH_3OCH_3+OH=CH_3OCH_2+H_2O$ is also of high importance for these types (the most important for jet-stirred reactor measurements) and the burner-stabilized flame experiments as well. Some reactions of the species $CH_2OCH_2O_2H$ and $CH_3OCH_2O_2$ are also of high importance for the flow reactor outlet concentration, jet-stirred reactor and rapid compression machine experiments, e.g. $CH_2OCH_2O_2H+O_2=O_2CH_2OCH_2O_2H$ and $CH_3OCH_2O_2=CH_2OCH_2O_2H$. Reactions including formaldehyde and formyl radical also appear between the most important reactions for several experiment types. Except for the flame experiments, the lists lack the reaction from the core subsystems, like the combustion of hydrogen and syngas, in comparison with other fuels like methane, methanol, ethanol or butanol where usually the $O_2+H=O+OH$ is the most sensitive reaction. Here, this only stands for the laminar burning velocity measurements, while it is in second place for burner-stabilized flame experiments (and also among the highest sensitivity coefficients for the shock tube experiments, but it is only 9th by frequency). Reactions of hydrogen peroxide, however, are of higher importance for the rapid compression machine experiments (e.g. $H_2O_2+M=OH+OH+M$ (LP)). The reactions of methyl radical were highly sensitive for shock tube experiments and for the flow reactor concentration-time profile measurements. The latter only includes a few data points corresponding to one experiment, which was the thermal decomposition of DME (pyrolysis). This is why the list of its most important reactions completely lacks steps with oxygen and the hydrogen oxidation system. The other experiment type that is very different from the others is the laminar burning velocity measurement in flames. Surprisingly, no DME reactions appeared between the 10 most important reactions (the first DME reaction was 13th with a frequency of 2%), but several reactions of formyl radical are present, e.g. $HCO+M=H+CO+M$ (LP) and $HCO+H=CO+H_2$, which are part of the DME oxidation system. It is also true that the sensitivity analysis was also performed for only a few data points due to the high running times, but the results indicate that it should be conducted for more points to see a clearer picture of the most important reaction steps.

Besides these experiments, the most important reactions are mostly in accordance with the results obtained by other researchers who performed local sensitivity analysis on DME combustion [8][27-28].

Table 3 Comparison of the sensitivity analysis results of the *A* preexponential factors of the 10 most sensitive reactions of the HPMech3.3-2018 mechanism. Freq.: The percentage number when the reaction had a higher absolute sensitivity coefficient than 10% of the largest absolute sensitivity coefficient of the given data point. In parenthesis: the overall number of data points used for the sensitivity analysis. $|\widetilde{sn}|_j$: mean of the scaled normalized absolute sensitivity coefficients. (LP): low pressure limit. (DUP): the given set of the duplicate Arrhenius-parameters.

	FR-OC			FR-CT		
		freq. (%)	$\lvert\widetilde{sn}\rvert_j$		freq. (%)	$\lvert\widetilde{sn}\rvert_j$
		(2274)			(17)	
1.	$CH_3OCH_3+HO_2 = CH_3OCH_2+H_2O_2$	51.1	0.223	$CH_3+CH_3OCH_3 = CH_4+CH_3OCH_2$	94.1	0.941
2.	$CH_3OCH_2O_2 = CH_2OCH_2O_2H$	50.4	0.171	$CH_3OCH_3+M = CH_3O+CH_3+M$	94.1	0.743
3.	$CH_3OCH_3+OH = CH_3OCH_2+H_2O$	47.9	0.368	$CH_3+CH_3+M = C_2H_6+M$	94.1	0.561
4.	$CH_2O+OH=HCO+H_2O$	46.2	0.264	$CH_3OCH_3+M = CH_3O+CH_3+M$ (LP)	82.4	0.109
5.	$CH_2OCH_2O_2H+O_2 = O_2CH_2OCH_2O_2H$	45.3	0.336	$CH_2O+CH_3 = HCO+CH_4$	76.5	0.223
6.	$CH_3+CH_3+M = C_2H_6+M$	41.8	0.257	$CH_3OCH_3+H = CH_3OCH_2+H_2$	5.9	0.038
7.	$CH_2OCH_2O_2H = OH+CH_2O+CH_2O$	40.4	0.243			
8.	$CH3OCH_2 = CH_3+CH_2O$	39.9	0.220			
9.	$CH3+CH_3OCH_3 = CH_4+CH_3OCH_2$	37.9	0.292			
10.	$CH_3+O_2 = CH_2O+OH$	34.5	0.084			
	JSR	(243)		IDT-ST	(929)	
1.	$CH_3OCH_3+OH = CH_3OCH_2+H_2O$	70.4	0.555	$CH_3+HO_2 = CH_3O+OH$	83.6	0.320
2.	$CH_2O+OH = HCO+H_2O$	67.1	0.342	$CH_3+HO_2 = CH_4+O_2$	81.3	0.262
3.	$CH_3OCH_3+HO_2 = CH_3OCH_2+H_2O_2$	66.3	0.369	$CH_3OCH_3+HO_2 = CH_3OCH_2+H_2O_2$	80.3	0.381
4.	$CH_2OCH_2O_2H+O_2 = O_2CH_2OCH_2O_2H$	50.2	0.356	$CH_3OCH_3+OH = CH_3OCH_2+H_2O$	79.5	0.215
5.	$CH_2OCH_2O_2H = OH+CH_2O+CH_2O$	44.9	0.272	$CH_2O+OH = HCO+H_2O$	74.3	0.209
6.	$HO_2+HO_2 = H_2O_2+O_2$ (DUP2)	44.9	0.133	$CH_3+CH_3+M = C_2H_6+M$	72.0	0.430
7.	$CH_3OCH_2O_2 = CH_2OCH_2O_2H$	41.6	0.211	$CH_2O+HO_2 = HCO+H_2O_2$	70.1	0.207
8.	$CH_3+CH_3+M = C_2H_6+M$	35.8	0.156	$CH_3OCH_3+M = CH_3O+CH_3+M$	69.0	0.397
9.	$H_2O_2+M = OH+OH+M$ (LP)	32.9	0.190	$H+O_2 = O+OH$	66.8	0.533
10.	$CH_3OCH_2 = CH_3+CH_2O$	32.5	0.138	$CH_2O+CH_3 = HCO+CH_4$	65.7	0.309
	IDT-RCM	(445)		BSF	(456)	
1.	$CH3OCH_2O_2 = CH_2OCH_2O_2H$	100.0	0.621	$HCO+M = H+CO+M$ (LP)	88.6	0.598
2.	$CH_3OCH_3+HO_2 = CH_3OCH_2+H_2O_2$	99.6	0.695	$H+O_2 = O+OH$	83.8	0.535
3.	$CH_2OCH_2O_2H+O_2 = O_2CH_2OCH_2O_2H$	95.5	0.792	$HCO+H = CO+H_2$	75.9	0.307
4.	$CH_2OCH_2O_2H = OH+CH_2O+CH_2O$	93.5	0.757	$CH_3OCH_3+OH = CH_3OCH_2+H_2O$	72.8	0.386
5.	$CH_3OCH_3+OH = CH_3OCH_2+H_2O$	92.8	0.743	$CH_3OCH_3+H = CH_3OCH_2+H_2$	70.4	0.463
6.	$CH_2O+OH = HCO+H_2O$	90.1	0.468	$HCO+O_2 = CO+HO_2$	64.9	0.198
7.	$H_2O_2+M = OH+OH+M$ (LP)	87.2	0.309	$CH_3OCH_3+M = CH_3O+CH_3+M$ (LP)	56.4	0.225
8.	$HO_2+HO_2 = H_2O_2+O_2$ (DUP1)	81.1	0.199	$CH_3+HO_2 = CH_3O+OH$	42.3	0.136
9.	$H_2O_2+M = OH+OH+M$	78.9	0.142	$CH_2O+H = HCO+H_2$	41.7	0.119
10.	$HO_2+HO_2 = H_2O_2+O_2$ (DUP2)	78.7	0.193	$CO+OH = CO_2+H$ (DUP1)	35.1	0.141
	LBV	(100)				
1.	$H+O_2 = O+OH$	100.0	1.000			
2.	$HCO+M = H+CO+M$ (LP)	100.0	0.349			
3.	$CH_3+H+M = CH_4+M$ (LP)	100.0	0.188			
4.	$HCO+H = CO+H_2$	87.0	0.158			
5.	$CO+OH = CO_2+H$ (DUP1)	82.0	0.382			
6.	$H+O_2+M=HO_2+M$ (LP)	77.0	0.233			
7.	$H_2+OH = H_2O+H$	56.0	0.098			
8.	$HCO+O_2 = CO+HO_2$	51.0	0.109			
9.	$HO_2+H = OH+OH$	51.0	0.096			
10.	$CH_3+HO_2 = CH_3O+OH$	46.0	0.100			

5. Conclusions

In the present study, 33149 data points in 1252 data series of 98 experimental articles corresponding to the combustion of dimethyl ether (neat DME, and DME mixtures containing hydrogen and/or carbon monoxide) were collected from the literature and simulated using 18 detailed reaction mechanisms with *Cantera* and *OpenSMOKE++* using simulation framework *Optima++*. The simulation results of different mechanisms were typically different from each other and the experimental data in several cases. The HPMech3.3-2018 mechanism had the best performance, followed by Zhao-2008 and Dai-2022. No mechanism could reproduce the experimental data within their 3σ uncertainty range on average, which means that more model development is necessary. The error distributions showed that most data points (about 75-80%) could be reproduced within this range by the models, and the remaining 20-25% percent led to these high averages. Local sensitivity analysis was carried out with the best-performing HPMech3.3-2018 using selected 4464 data points. The most important reactions were investigated by experiment types. The most important steps include DME reactions with several species, formaldehyde, formyl and methyl radical reactions and reactions from the hydrogen oxidation system. For most experiments, the most important reactions are in accordance with the findings of other authors. For the LBV experiments, surprising results were obtained, which require further investigations.

Declaration of competing interest

The authors declare that they have no known competing financial interests or personal relationships that could have appeared to influence the work reported in this paper.

Acknowledgements

The authors acknowledge the support of the NKFIH grant OTKA K147024 of the Hungarian National Research, Development and Innovation Office and CYPHER CA22151 COST Action, which is supported by COST (European Cooperation in Science and Technology). ÁVR was also supported by the DKOP-23 Doctoral Excellence Program of the Ministry for Culture and Innovation of Hungary from the source of the National Research, Development, and Innovation Fund.

References

[1] C. Arcoumanis, C. Bae, R. Crookes, E. Kinoshita, The potential of di-methyl ether (DME) as an alternative fuel for compression-ignition engines: A review, Fuel 87 (2008), 1014-1030.

[2] T. Turányi, T. Nagy, I. G. Zsély, M. Cserháti, T. Varga, B. T. Szabó, I. Sedyó, P. T. Kiss, A. Zempléni, H. J. Curran, Determination of rate parameters based on both direct and indirect measurements, Int. J. Chem. Kinet. 44 (2012) 284–302.

[3] T. Varga, C. Olm, M. Papp, Á. Busai, A. Gy. Szanthoffer, I. Gy. Zsély, T. Nagy, T. Turányi, ReSpecTh Kinetics Data Format Specification v2.5, Chemical Kinetics Laboratory, ELTE Institute of Chemistry (2024).

[4] M. Papp, T. Varga, Á. Busai, I. Gy. Zsély, T. Nagy, T. Turányi: Optima++ v2.5: A general C++ framework for performing combustion simulations and mechanism optimization (2024); available at http://respecth.hu/ (Accessed March 2025).

[5] D. G. Goodwin, H. K. Moffat, I. Schoegl, R. L. Speth, B. W. Weber. Cantera: An object-oriented software toolkit for chemical kinetics, thermodynamics, and transport processes (2023). https://www.cantera.org (Accessed March 2025).

[6] A. Cuoci, A. Frassoldati, T. Faravelli, E. Ranzi, *OpenSMOKE++:* An object-oriented framework for the numerical modeling of reactive systems with detailed kinetic mechanisms, Comput. Phys. Commun. 192 (2015) 237–264.

[7] H. J. Curran, S. L. Fischer, F. L. Dryer, The reaction kinetics of dimethyl ether. II: Low-temperature oxidation in flow reactors. Int. J. Chem. Kinet., 32 (2000) 741-759.

[8] U. Burke, K. P. Somers, P. O'Toole, C. M. Zinner, N. Marquet, G. Bourque, E. L. Petersen, W. K. Metcalfe, Z. Serinyel, H. J. Curran, An ignition delay and kinetic modeling study of methane, dimethyl ether, and their mixtures at high pressures, Combust. Flame 162 (2015) 315-330.

[9] C. B. Reuter, R. Zhang, O. R. Yehia, Y. Rezgui, Y. Ju, Counterflow flame experiments and chemical kinetic modeling of dimethyl ether/methane mixtures, Combustion and Flame, 196 (2018) 1-10.

[10] Z. Zhao, M. Chaos, A. Kazakov, F. L. Dryer, Thermal decomposition reaction and a comprehensive kinetic model of dimethyl ether, Int. J. Chem. Kinet., 40 (2008) 1-18.

[11] L. Dai, L. Lu, C. Zou, Q. Lin, W. Xia, H. Shi, J. Luo, C. Peng, S. Wang, An improved low and high-temperature dimethyl ether kinetic model for the combustion atmospheres with high CO2 concentration, Combust. Flame 238 (2022) 111922.

[12] NUI Galway Combustion Chemistry Centre, AramcoMech 2.0, 2017, http://www.nuigalway.ie/combustionchemistrycentre/mechanismdownloads/aramcomech20/ (accessed March 2025)

[13] Z. Wang, X. Zhang, L. Xing, L. Zhang, F. Herrmann, K. Moshammer, F. Qi, Katharina Kohse-Höinghaus, Experimental and kinetic modeling study of the low- and intermediate-temperature oxidation of dimethyl ether, Combust. Flame 162 (2015) 1113-1125.

[14] C.-W. Zhou, Y. Li, U. Burke, C. Banyon, K. P. Somers, S. Ding, S. Khan, J. W. Hargis, T. Sikes, O. Mathieu, E. L. Petersen, M. AlAbbad, A. Farooq, Y. Pan, Y. Zhang, Z. Huang, J. Lopez, Z. Loparo, S. S. Vasu, et al., An experimental and chemical kinetic modeling study of 1,3-butadiene combustion: Ignition delay time and laminar flame speed measurements, Combust. Flame 197 (2018) 423–438.

[15] S. Panigrahy, J. Liang, S. S. Nagaraja, Z. Zuo, G. Kim, S. Dong, G. Kukkadapu, W. J. Pitz, S. S. Vasu, H. J. Curran,

A comprehensive experimental and improved kinetic modeling study on the pyrolysis and oxidation of propyne, Proc. Comb. Inst. 38 (2021) 479-488.
[16] M. Pelucchi, S. Schmitt, N. Gaiser, A. Cuoci, A. Frassoldati, H. Zhang, A. Stagni, P, Oßwald, K. Kohse-Höinghaus, T. Faravelli, On the influence of NO addition to dimethyl ether oxidation in a flow reactor, Combust. Flame 257 (2023) 112464.
[17] W. K. Metcalfe, S. M. Burke, S. S. Ahmed, H. J. Curran, A hierarchical and comparative kinetic modeling study of C1 - C2 hydrocarbon and oxygenated fuels, Int. J. Chem. Kinet. 45 (2013) 638–675.
[18] L-S. Tran, Y. Li, M. Zeng, J. Pieper, F. Qi, F. Battin-Leclerc, K. Kohse-Höinghaus, O. Herbinet, Elevated pressure low-temperature oxidation of linear five-heavy-atom fuels: diethyl ether, -pentane, and their mixture. Zeitschrift für Physikalische Chemie 234 (2020) 1269–1293.
[19] K. P. Shrestha, S. Eckart, A. M. Elbaz, B. R. Giri, C. Fritsche, L. Seidel, W. L. Roberts, H. Krause, F. Mauss, A comprehensive kinetic model for dimethyl ether and dimethoxymethane oxidation and NOx interaction utilizing experimental laminar flame speed measurements at elevated pressure and temperature, Combus. Flame 218 (2020) 57-74.
[20] D. Liu, J. Santner, C. Togbé, D. Felsmann, J. Koppmann, A. Lackner, X. Yang, X. Shen, Y. Ju, K. Kohse-Höinghaus, Flame structure and kinetic studies of carbon dioxide-diluted dimethyl ether flames at reduced and elevated pressures, Combust. Flame 160 (2013) 2654-2668.
[21] E. W. Kaiser, T. J. Wallington, M. D. Hurley, J. Platz, H. J. Curran, W. J. Pitz, C. K. Westbrook, Experimental and Modeling Study of Premixed Atmospheric-Pressure Dimethyl Ether−Air Flames, J. Phys. Chem. A 104 (2000) 8194-8206.
[22] W. Huang, Q. Zhao, Z. Huang, H. J. Curran, Y. Zhang, A kinetics and dynamics study on the auto-ignition of dimethyl ether at low temperatures and low pressures, Proc. Comb. Inst. 38 (2021) 601-609.
[23] G. Issayev, B. R. Giri, A. M. Elbaz, K. P. Shrestha, F. Mauss, W. L. Roberts, A. Farooq, Combustion behavior of ammonia blended with diethyl ether, Proceedings of the Combustion Institute 38 (2021) 499-506.
[24] H. Hashemi, J. M. Christensen, P. Glarborg, High-pressure pyrolysis and oxidation of ethanol, Fuel 218 (2018) 247-257.
[25] K. Yasunaga, F. Gillespie, J. M. Simmie, H. J. Curran, Y. Kuraguchi, H. Hoshikawa, M. Yamane, and Y. Hidaka, A Multiple Shock Tube and Chemical Kinetic Modeling Study of Diethyl Ether Pyrolysis and Oxidation, J. Phys. Chem. A 114 (2010) 9098-9109.
[26] T. Turányi, A. S. Tomlin, Analysis of Kinetic Reaction Mechanisms; Springer, 2014.
[27] L. Marrodán, Á. J. Arnal, Á. Millera, R. Bilbao, M. U. Alzueta, The inhibiting effect of NO addition on dimethyl ether high-pressure oxidation, Combust. Flame 197 (2018) 1-10.
[28] X. Jiang, F. Deng, F. Yang, Y. Zhang, Z. Huang, High temperature ignition delay time of DME/n-pentane mixture under fuel lean condition, Fuel 191 (2017) 77-86.